

Determination of the orientation of C₆₀ adsorbed on Au(111) and Ag(111)

Eric I. Altman and Richard J. Colton

Chemistry Division, Code 6177, Naval Research Laboratory, Washington, D.C. 20375-5342

(Received 25 June 1993)

Adsorbate bonding and preferred adsorption sites and rotational orientations of C₆₀ on Au(111) and Ag(111) were studied using scanning tunneling microscopy (STM) and related techniques. Spatially resolved tunneling spectroscopy and barrier height measurements indicated that bonding occurs by charge transfer from the metal to C₆₀. The internal structure of adsorbed C₆₀ observed by STM was found to be a strong function of the adsorption site, the molecular orientation, and the tunneling bias. Occupied state images were found to reflect the adsorption site symmetry while unoccupied state images reflected the molecular symmetry. In domains where all the molecules were in equivalent adsorption sites, the observed internal structure of adsorbed C₆₀ was assigned to an on-top site with the five-membered ring on the surface.

I. INTRODUCTION

We have been using ultrahigh vacuum scanning tunneling microscopy/spectroscopy (UHV-STM/S) to study the nucleation, growth, and structure of C₆₀ films and fullerene films on noble-metal surfaces because many potential applications of these materials depend on surface interactions and the use of thin films.¹⁻³ The Au(111) surface was initially chosen for these studies because it undergoes an unusual reconstruction that acts as an ordered array of nucleation sites for the growth of metal films.⁴ The behavior of C₆₀ on Au(111) and Ag(111) was compared because Ag(111) has the same lattice constant and nearly the same electronic structure as Au(111) but does not reconstruct.

Our previous studies indicated unusual and potentially important surface interactions. First, it was found that C₆₀ interacts strongly (50–60 kcal/mol estimated heat of adsorption) even with generally inert Au and Ag surfaces.^{1,3} Since stronger interactions are expected for more reactive metals such as Ni and Pt, this suggests that the fullerenes can be derivatized through metal catalysis (e.g., hydrogenation). Second, STM images showed contrast variations between adsorbed C₆₀ molecules even when all the molecules were in equivalent sites.^{2,3} Tunneling spectroscopy images indicated that these contrast variations were due to electronic differences and not to topography. Second-layer molecules appeared uniform indicating that the interaction with the substrate was responsible for the contrast variations. Further, it was found for both Ag(111) and Au(111) that the same molecule in the same position on the surface could reversibly change contrast from bright to dim. Together, these results indicated that the observed contrast variations were due to variations in substrate-adsorbate bonding due to molecules bound in different rotational orientations on the surface (e.g., five-membered vs six-membered ring on the surface). This paper focuses on identifying these rotational orientations and adsorption sites for C₆₀ on Au(111) and Ag(111) using occupied and unoccupied state STM measurements, and on determining the nature

of the surface-C₆₀ bond using spatially resolved tunneling spectroscopy and barrier height measurements. The results demonstrate how adsorption site geometry and surface interactions influence the appearance of adsorbed molecules in STM.

II. EXPERIMENT

The experimental equipment and procedures used in this study have been described in detail previously.^{1-3,5} Briefly, C₆₀ was sublimed onto room-temperature metal surfaces in UHV by heating to 400 °C. The C₆₀ films were characterized *in situ* by STM, low-energy electron diffraction (LEED), and Auger-electron spectroscopy (AES). *Ex situ* time-of-flight secondary-ion mass spectrometry (TOF-SIMS) was used to determine the composition of the fullerene films.

Epitaxial (111) oriented Au and Ag films on mica were used as substrates. Prior to C₆₀ deposition, these substrates were cleaned by cycles of Ar ion sputtering and annealing to 600 °C until AES showed no traces of impurities, a sharp LEED pattern was obtained, and STM images showed large areas (0.01 μm²) free of impurities.

Atomic-resolution STM images of uncovered areas of the substrate were used to determine the orientation of the adlayer with respect to the substrate. The tunneling bias required to image the substrate atoms was different from that required to image C₆₀, making it impossible to determine the adsorption sites directly with STM. It will be demonstrated that the observed C₆₀ internal structures are not due to tip artifacts, even though internal structure could not be resolved in every STM image.

III. RESULTS AND DISCUSSION

Previously, we reported that C₆₀ forms two close-packed adsorbate phases on Au(111):¹ a structure with roughly 38×38 periodicity in which the crystallographic directions of the overlayer match those of the substrate and the lattice matching is poor, and a 2√3×2√3 R30° structure with nearly perfect lattice matching (less than

0.4% mismatch) in which all the molecules are in equivalent surface sites. In both phases the C_{60} spacing is 1.0 nm, the same as the (111) spacing in bulk fcc C_{60} . The internal structure observed with STM did not correspond to the atom positions in the C_{60} molecule in either phase. As shown in the occupied state image [-2 V bias (sample negative)] in Fig. 1(a), adsorbed C_{60} in $2\sqrt{3}\times 2\sqrt{3}$ $R30^\circ$ domains appear as either hexagons with holes in the center or as brighter (or apparently 0.09-nm-higher) molecules without holes. Previously, we showed using TOF-SIMS that the films contained only C_{60} and so the brighter molecules are not due to larger fullerenes. The

contrast variations also cannot be due to different adsorption sites (e.g., on-top vs threefold-hollow) because the lattice matching in $2\sqrt{3}\times 2\sqrt{3}$ $R30^\circ$ domains requires that all the molecules be in equivalent sites. Tunneling spectroscopy images indicated that the appearance of bright and dim molecules in the STM images is due to electronic differences caused by surface interactions.^{2,3} STM images of 38×38 domains showed a greater variety of internal structures including striped structures and “X” shaped structures, as shown in the occupied state images in Figs. 1(b) and 1(c). Others have reported similar observations for C_{60} on Au(110) and polycrystalline

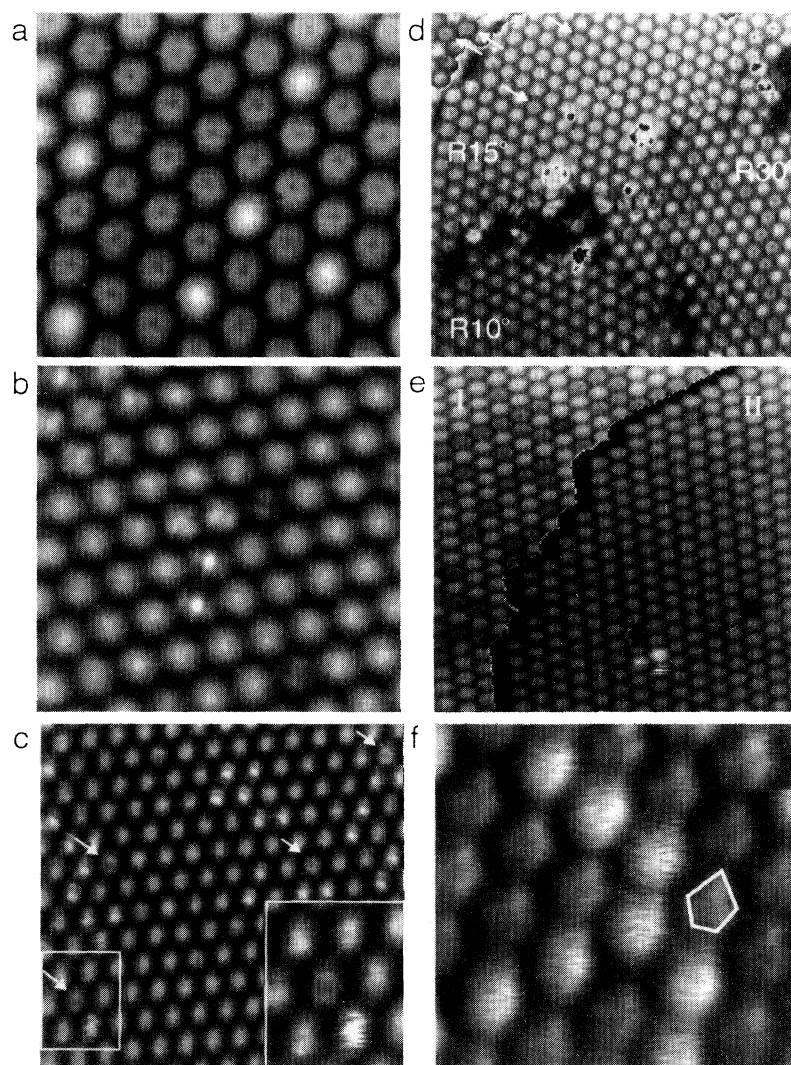


FIG. 1. (a) Occupied state STM image of a $2\sqrt{3}\times 2\sqrt{3}$ $R30^\circ$ C_{60} domain on Au(111) [7.3×7.3 nm, -2 V bias (sample negative)]. (b) Occupied state image of a 38×38 C_{60} domain on Au(111) (9.1×9.1 nm, -2 V). (c) Occupied state image of a 38×38 C_{60} domain on Au(111) (13×13 nm, -2.25 V). The inset shows the boxed area enlarged. The arrows point to hexagonal shaped molecules with holes in the center. (d) Occupied state image of a C_{60} monolayer on Ag(111) showing three different domains (19×19 nm, -2 V). The arrows in the $R15^\circ$ domain point to molecules that display internal structure similar to that observed in $2\sqrt{3}\times 2\sqrt{3}$ $R30^\circ$ domains. (e) Occupied state image of first- and second-layer C_{60} molecules in a $2\sqrt{3}\times 2\sqrt{3}$ $R30^\circ$ domain on Ag(111) (20×20 nm, -2.5 V). The I and II indicate the first and second layer, respectively. The step height has been subtracted from the upper terrace to enhance the contrast. (f) Unoccupied state image of a $2\sqrt{3}\times 2\sqrt{3}$ $R30^\circ$ C_{60} domain on Au(111) (4.8×4.8 nm, 1.5 V). The outline is drawn to emphasize the pentagonal shape of the molecule and its orientation.

Au.^{6,7} STM images of 38×38 domains also revealed that the same patterns were always aligned in the same direction with respect to the underlying substrate. These results suggest that the observed internal structures depend on the geometry of the adsorption site and the orientation of the molecule. If the internal structure shown in Fig. 1(a) is due to a specific adsorption site and rotational orientation, then the same structure should be observed in 38×38 domains at positions where the molecules fall in the same registry as the $2\sqrt{3} \times 2\sqrt{3}$ $R 30^\circ$ structure and are properly oriented. As shown in Fig. 1(c), this is in fact the case. In this figure, the arrows point to a few isolated hexagons with holes; the same structure that predominates in Fig. 1(a). Further, comparing the inset in Fig. 1(c) with 1(a) reveals that the corners of the hexagons align with the close-packed directions of the Au(111) substrate. This suggests that the hexagonal shape of the molecule is not due to the packing symmetry but to local variations in electronic state density around the adsorbed molecule.

Results for Au(111) were compared with those for Ag(111), which has nearly the same lattice constant (0.289 nm vs 0.288 nm for Au) and electronic structure as Au but is somewhat more reactive. Figure 1(d) shows an occupied state image with three different first-layer domains. [On Ag(111) nearly all large domains were $2\sqrt{3} \times 2\sqrt{3}$ $R 30^\circ$ but occasionally small domains with other orientations were observed near steps.³] The $2\sqrt{3} \times 2\sqrt{3}$ $R 30^\circ$ domain again shows hexagons with holes in the center and brighter molecules without holes. The only difference apparent between images of $2\sqrt{3} \times 2\sqrt{3}$ $R 30^\circ$ domains on Au(111) and Ag(111) is a higher density of brighter molecules on the Ag(111) surface. In the two other domains, and particularly at the

domain boundaries, mostly striped structures are observed. In addition, a low density of hexagonal structures with holes in the center is seen in the $R 15^\circ$ domain. This demonstrates that the phenomena shown in Figs. 1(a) and 1(b) can be observed in the same image with the same tip indicating that these results are not due to tip effects. The remainder of this paper will focus on $2\sqrt{3} \times 2\sqrt{3}$ $R 30^\circ$ domains because the molecules lie in equivalent adsorption sites in this phase offering a greater opportunity to assign observed internal structures to specific bonding configurations.

Images of second-layer molecules also support the conclusion that the observed internal structures are influenced by the adsorption site and by bonding to the surface. Figure 1(e) shows first- and second-layer molecules on Ag(111). The first layer appears similar to Fig. 1(a), but second-layer molecules appear uniform with no internal structure because the molecules are not interacting with the metal surface and are presumably rotating at the bulk rate of 10^9 sec^{-1} .⁸ In addition, the uniform appearance of the second layer supports contrast variations in the first layer due to electronic differences rather than topographic differences. If the contrast variations were due to height differences then similar height variations would be expected in the second layer.

The observed internal structures were found to depend on tunnel bias. Figure 1(f) shows an unoccupied state image (+1.5 V bias) of a $2\sqrt{3} \times 2\sqrt{3}$ $R 30^\circ$ C_{60} monolayer on Au(111). Comparing Fig. 1(f) with 1(a), no hole is seen in the unoccupied state image and a difference in shape is apparent. Figure 1(f) suggests a pentagonal shape rather than the hexagonal shape seen in occupied state images. These results are not due to tip effects as illustrated in Figs. 2(a) and 2(b), which show the same results for

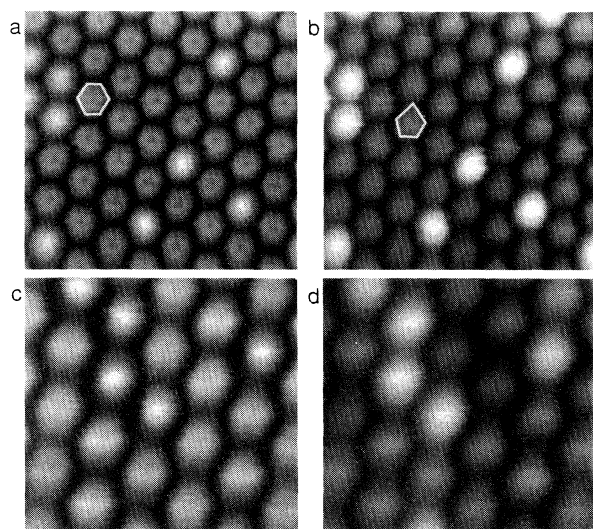


FIG. 2. (a) and (b) Simultaneously acquired occupied (-2 V) and unoccupied (1.5 V) state images of $2\sqrt{3} \times 2\sqrt{3}$ $R 30^\circ$ C_{60} domains on Au(111) (7.3×7.3 nm). The outlines are drawn to emphasize the hexagonal shape of the molecules in (a) and the pentagonal shape in (b). (c) and (d) same as (a) and (b) except images acquired at -1.25 and 1.25 V (4.8×4.8 nm).

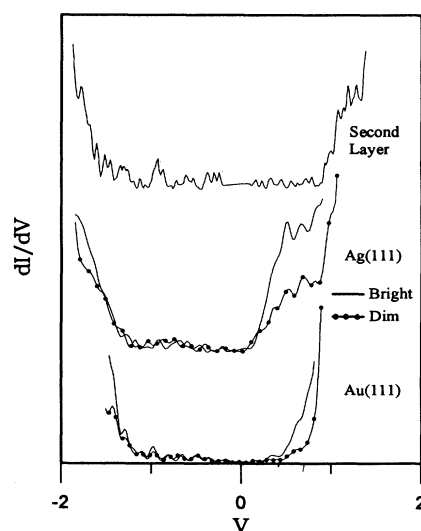


FIG. 3. Tunneling spectra for second-layer C_{60} molecules on Ag(111) and first-layer molecules on Au(111) and Ag(111). Bright and dim refer to spectra recorded over molecules that appear bright or dim in topographic images recorded simultaneously with the tunneling spectra. The spectra are plotted as dI/dV vs V in volts.

simultaneously acquired occupied (-2 V bias) and unoccupied state ($+1.5$ V bias) images, although the shape in the unoccupied state image is not as sharp as that in Fig. 1(f). Figures 2(a) and 2(b) also indicate a greater apparent height difference between bright and dim molecules in unoccupied state images [0.11 nm in Fig. 2(b) compared to 0.09 nm in Fig. 2(a)]. Reducing the bias (or imaging closer to the Fermi level) also affected the observed internal structures. As shown in Fig. 2(d), on the occupied side reducing the bias to 1.25 V causes minor changes; the shapes become less distinct but the contrast between bright and dim molecules is unaffected. On the occupied side, however, greater changes were observed. Figure 2(c), which was obtained simultaneously with Fig. 2(d), shows that reducing the bias to -1.25 V causes the holes to fill and the apparent height difference between the bright and dim molecules to decrease but does not appear to affect the shape. The above results are all for C₆₀ on Au(111); similar results were obtained for Ag(111).

To understand the observed intramolecular contrast and its dependence on tunnel bias, the electronic structure of the molecule and the bonding to the surface must be considered. Tunneling spectra indicate bonding involves charge transfer from the metal to the molecule. In Fig. 3, the spectra of first-layer molecules are considerably different from the spectra for second-layer molecules, which are expected to be more bulklike. The band gap is reduced from over 1 eV for the second layer to less than 0.2 eV for the first layer on Au and to approximately 0 eV on Ag. The gap narrowing is due to broadening of C₆₀ states upon adsorption and to a contribution of the underlying metal to the tunnel current. In particular, the unoccupied state density is shifted closer to the Fermi level for the monolayer on both Au and Ag. Comparatively small shifts are observed in the occupied states. These results are similar to ultraviolet and inverse photoelectron spectroscopy (UPS and IPS) data reported for C₆₀ on polycrystalline Au.⁹ Shifts towards lower energy in the unoccupied states for the monolayer compared to C₆₀ multilayers were observed with IPS while UPS indicated little difference in the occupied states between monolayers and multilayers. The shift in the unoccupied states was attributed to charge transfer to the molecule causing lowest-unoccupied-molecular-orbital (LUMO) hybridization and partial filling of LUMO derived states. The interaction was not considered strong enough to al-

ter the icosahedral symmetry of the molecule and the LUMO-derived states are expected to have the symmetry of the LUMO. As shown in Fig. 3, larger shifts were observed on Ag(111) suggesting a stronger interaction with the more reactive surface. Barrier height measurements support bonding by charge transfer to the molecule. As shown in Fig. 4 for C₆₀ on Ag(111) [Au(111) gave similar results], barrier height images indicate a higher barrier height (by 1.6 eV) over C₆₀ molecules compared to the bare metal.

Comparison of tunneling spectra taken over bright and dim first-layer molecules on Ag(111) and Au(111) also showed much greater differences in the unoccupied states than in the occupied states. This explains why greater contrast variations between adsorbed C₆₀ molecules are observed in unoccupied state images. For Au(111), the difference between the bright and dim spectra appears as an energy shift. The spectrum at the dimmer molecules is similar to that obtained for the second layer suggesting that dimmer molecules are more weakly bound to the surface. On Ag(111), however, the difference is better characterized as a change in peak intensity. It is not clear why a shift is observed in one case and a change in intensity in the other, however, on both surfaces the difference between bright and dim molecules manifests itself mainly in the LUMO, the state involved in bonding to the surface.

Given the large differences in adsorbate bonding between bright and dim molecules, one might expect the molecules to uniformly adsorb in the orientation that yields the strongest bond to the surface. However, the adsorption energy depends on the interaction between neighboring adsorbed molecules in addition to the strength of the substrate-adsorbate bond. For C₆₀ on Au(111) and Ag(111) the adsorbate interactions appear to be attractive because isolated C₆₀ molecules are never observed on Au(111) and Ag(111) at room temperature; the molecules form close-packed chains at the steps and close-packed layers on the terraces even at the lowest coverages.^{1,3} Further, for bulk C₆₀ it is known that certain orientations of neighboring molecules are favored.¹⁰ In the orientationally ordered phase that occurs below 260 K the double bonds between two hexagons point to the face of a pentagon on the neighboring molecule.^{8,10} Therefore, the energy of an adsorbed C₆₀ molecule depends on the number of nearest neighbors and the orientation of the neighbors in addition to the strength of the metal-adsorbate bond. The observation of different orientations at room temperature suggests that variations in substrate-adsorbate bond strength and the sum of the molecule-molecule interactions with orientation are of a similar magnitude. The higher density of brighter molecules on Ag(111) compared to Au(111) suggests a stronger interaction with the more reactive Ag surface. That is, on Ag(111) the metal-adsorbate bond makes a larger contribution to the total energy of the adsorbed molecule favoring orientations that give rise to bright molecules in STM images. Previously, we reported other evidence that C₆₀ adsorbs more strongly to Ag(111) than to Au(111) but that the difference was not large.³

Only the highest occupied molecular orbital (HOMO)

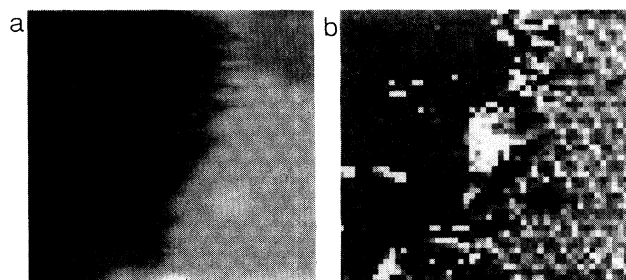


FIG. 4. Simultaneously obtained topographic (a) and barrier height (b) images of C₆₀ on Ag(111). The average barrier height is 3.4 eV over the bare metal and 5.0 eV over the C₆₀ molecules.

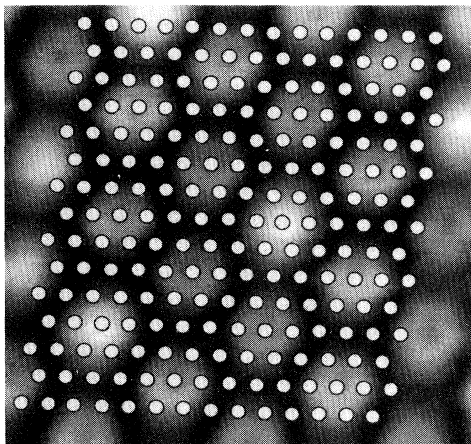


FIG. 5. Occupied state image of (4.8×4.8 nm, -2 V). The circles represent the positions of the underlying Au atoms for C_{60} in on-top sites. The Au lattice has been slightly skewed to account for thermal drift in the image.

and LUMO are accessible in the bias voltage ranges used in this study and, therefore, only these states need to be considered to understand the STM images showing internal structure in Figs. 1(a), 1(f), and 2(a)–2(d). Calculations indicate that the C_{60} LUMO is concentrated in the single bonds between a hexagon and a pentagon while the HOMO is concentrated in the double bonds between two hexagons.¹¹ The occupied state images, Figs. 1(a), 1(d), 1(e), 2(a), and 2(c), indicate sixfold symmetry for the HOMO. However, the molecule does not have any sixfold axis, only 2, 3, and 5. Further, the symmetry of the arrangement of the double bonds is always the same as that of the single bonds, independent of the orientation. Therefore, the observed differences in symmetry between occupied and unoccupied state images cannot be explained by the molecular states alone. For these reasons the symmetry of the adsorption site must also be considered. Since the tunneling spectra show states due to the metal between the first molecular state [centered at ~ 2.2 eV (Ref. 9)] and the Fermi level and because the first occupied state is much further from the Fermi level than is the first unoccupied state (see Fig. 3), at similar biases occupied state images should contain a greater contribution from the underlying metal than unoccupied state images. Therefore, the occupied state images may reflect the symmetry of the adsorption site while the unoccupied state images reflect the symmetry of the molecular states. The hexagonal symmetry of the occupied state images suggest an on-top site, the only surface site that gives sixfold symmetry (not considering differences between fcc and hcp type hollows). Figure 5 shows that for on-top sites the corners of the hexagons

coincide with the Au atom positions. This, however, does not explain the hole in the center. The hole filling when the bias was decreased (or moved further from the molecular state) suggests that a node in the molecular states is responsible for the hole.

The apparent pentagonal shape of the molecules in the unoccupied state images shown in Figs. 1(f) and 2(b) suggests fivefold symmetry for the LUMO. Considering only the atoms visible from the top, the only way to orient the molecule to give a fivefold symmetric arrangement of single bonds is with the five-membered ring on the surface. In terms of the adsorbate bonding, putting the five-membered ring on the surface is reasonable because this places the charge deficient part of the molecule on the surface to accept charge from the metal. Also, since the density of the HOMO is lowest in the five-membered rings, putting the five-membered ring on the surface is consistent with the hole in the center of the molecule observed in occupied state images.

IV. CONCLUSIONS

We have shown that (i) the internal structure of adsorbed C_{60} observed with STM depends on the adsorption site, and the electronic structure and rotational orientation of the molecule, (ii) C_{60} bonds to Au and Ag surfaces by charge transfer from the surface to the molecule, and (iii) the degree to which the substrate and molecular structure contribute to the STM image can be varied by changing the tunneling bias. Based on the symmetry of the occupied and unoccupied state STM images and the symmetry of the molecular orbitals we have attributed the observed internal structure of C_{60} adsorbed on metal surfaces to a specific surface site and molecular orientation, namely an on-top site with the five-membered ring on the surface. The results also elucidate the factors influencing the appearance of adsorbed molecules in STM in general. Others have reported that the symmetry of an adsorbed molecule observed with STM can be affected by the substrate,¹² however, this is the first time, to our knowledge, it has been shown that the same molecule in the same image can appear different because of variations in molecular orientation and adsorption site. The results also show the importance of tunneling spectroscopy, barrier height imaging, and multiple bias imaging to understanding STM images of adsorbed molecules.

ACKNOWLEDGMENTS

E.I.A. acknowledges the support of ASEE through the Office of Naval Research (ONR). We also acknowledge helpful discussions with D. P. DiLella, L. J. Whitman, B. I. Dunlap, S. M. Hues, and J. A. Harrison. This work was supported by ONR.

- ¹E. I. Altman and R. J. Colton, *Surf. Sci.* **279**, 49 (1992).
- ²E. I. Altman and R. J. Colton, in *Atomic and Nanoscale Modification of Materials: Fundamentals and Applications*, Vol. E239 of NATO Advanced Study Institute, Series E: Applied Sciences, edited by P. Avouris (Plenum, New York, 1993), p. 303.
- ³E. I. Altman and R. J. Colton, *Surf. Sci.* **295**, 13 (1993).
- ⁴D. D. Chambliss and R. J. Wilson, *J. Vac. Sci. Technol. B* **9**, 928 (1991); D. D. Chambliss, R. J. Wilson, and S. Chiang, *Phys. Rev. Lett.* **190**, 1721 (1991); *J. Vac. Sci. Technol. B* **9**, 933 (1991).
- ⁵E. I. Altman, D. P. DiLella, J. Ibe, K. Lee, and R. J. Colton, *Rev. Sci. Instrum.* **64**, 1239 (1993).
- ⁶T. Chen, S. Howells, M. Gallagher, L. Yi, D. Sarid, D. L. Lichtenberger, K. W. Nebesney, and C. D. Ray, *J. Vac. Sci. Technol. B* **10**, 170 (1992).
- ⁷Y. Zhang, X. Gao, and M. J. Weaver, *J. Phys. Chem.* **96**, 510 (1992).
- ⁸D. A. Neumann, J. R. D. Copley, R. I. Cappelletti, W. A. Kamitakahara, R. M. Lindstrom, K. M. Creegan, D. M. Cox, W. J. Romanow, N. Coustel, J. P. McCauley, Jr., N. C. Maliszewskij, J. E. Fischer, and A. B. Smith III, *Phys. Rev. Lett.* **67**, 3808 (1991).
- ⁹T. R. Ohno, Y. Chen, S. E. Harvey, G. H. Kroll, J. H. Weaver, R. H. Hauffer, and R. E. Smalley, *Phys. Rev. B* **44**, 13 747 (1991).
- ¹⁰W. I. F. David, R. M. Ibberson, J. C. Matthewman, K. Prasad, T. J. S. Dennis, J. P. Hare, H. W. Kroto, R. Taylor, and D. R. M. Walton, *Nature* **353**, 147 (1991).
- ¹¹M. B. Jost, N. Troullier, D. M. Poirier, J. L. Martins, J. H. Weaver, L. P. F. Chibante, and R. E. Smalley, *Phys. Rev. B* **44**, 1966 (1991); N. Troullier and J. L. Martins, *ibid.* **46**, 1754 (1992).
- ¹²H. Ohtani, R. J. Wilson, S. Chiang, and C. M. Mate, *Phys. Rev. Lett.* **60**, 2398 (1988).

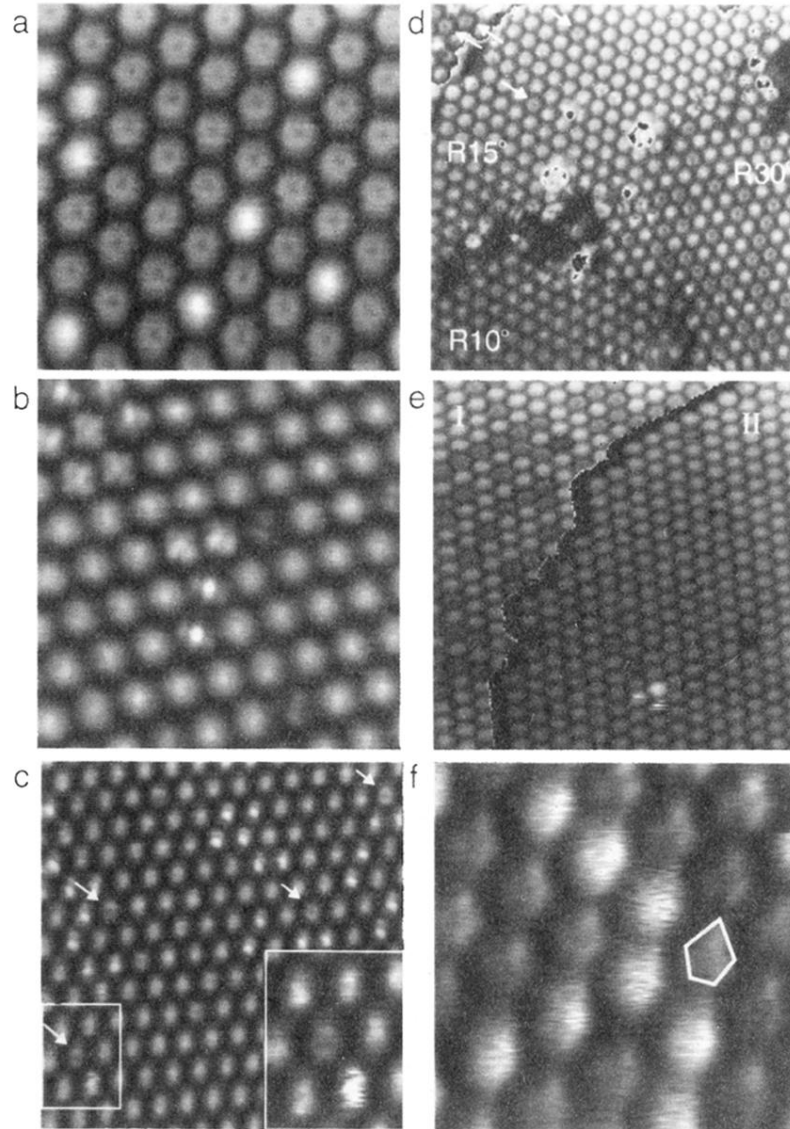


FIG. 1. (a) Occupied state STM image of a $2\sqrt{3} \times 2\sqrt{3}$ $R30^\circ$ C_{60} domain on Au(111) [7.3×7.3 nm, -2 V bias (sample negative)]. (b) Occupied state image of a 38×38 C_{60} domain on Au(111) (9.1×9.1 nm, -2 V). (c) Occupied state image of a 38×38 C_{60} domain on Au(111) (13×13 nm, -2.25 V). The inset shows the boxed area enlarged. The arrows point to hexagonal shaped molecules with holes in the center. (d) Occupied state image of a C_{60} monolayer on Ag(111) showing three different domains (19×19 nm, -2 V). The arrows in the $R15^\circ$ domain point to molecules that display internal structure similar to that observed in $2\sqrt{3} \times 2\sqrt{3}$ $R30^\circ$ domains. (e) Occupied state image of first- and second-layer C_{60} molecules in a $2\sqrt{3} \times 2\sqrt{3}$ $R30^\circ$ domain on Ag(111) (20×20 nm, -2.5 V). The I and II indicate the first and second layer, respectively. The step height has been subtracted from the upper terrace to enhance the contrast. (f) Unoccupied state image of a $2\sqrt{3} \times 2\sqrt{3}$ $R30^\circ$ C_{60} domain on Au(111) (4.8×4.8 nm, 1.5 V). The outline is drawn to emphasize the pentagonal shape of the molecule and its orientation.

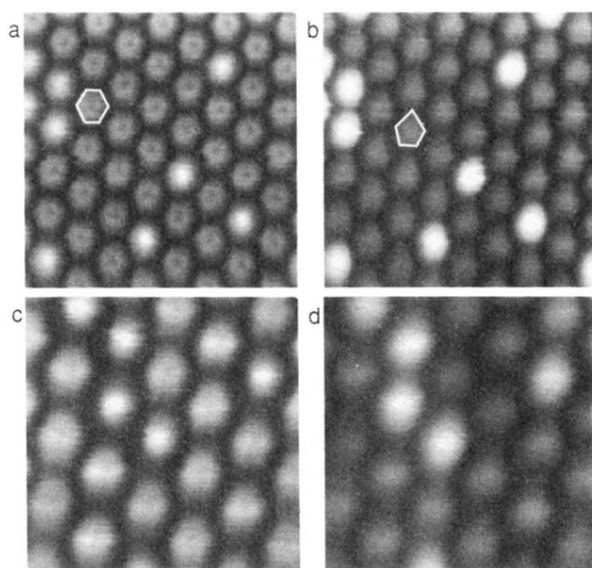


FIG. 2. (a) and (b) Simultaneously acquired occupied (-2 V) and unoccupied (1.5 V) state images of $2\sqrt{3}\times 2\sqrt{3}$ $R30^\circ$ C_{60} domains on Au(111) (7.3×7.3 nm). The outlines are drawn to emphasize the hexagonal shape of the molecules in (a) and the pentagonal shape in (b). (c) and (d) same as (a) and (b) except images acquired at -1.25 and 1.25 V (4.8×4.8 nm).

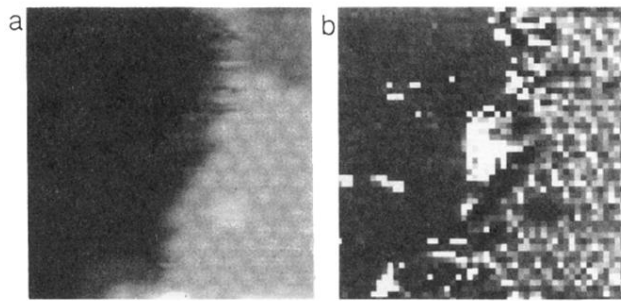


FIG. 4. Simultaneously obtained topographic (a) and barrier height (b) images of C_{60} on Ag(111). The average barrier height is 3.4 eV over the bare metal and 5.0 eV over the C_{60} molecules.

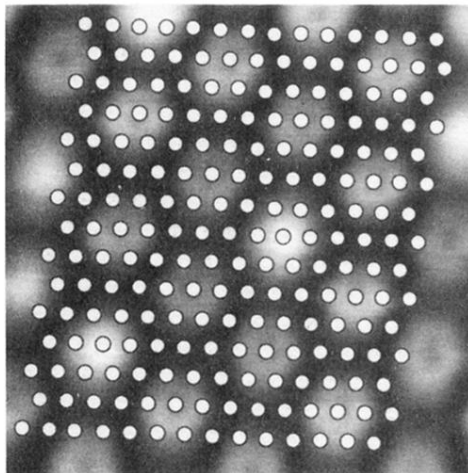


FIG. 5. Occupied state image of (4.8×4.8 nm, -2 V). The circles represent the positions of the underlying Au atoms for C_{60} in on-top sites. The Au lattice has been slightly skewed to account for thermal drift in the image.